



# Degradation of pesticides present in tomato rinse water by direct photolysis and UVC/H<sub>2</sub>O<sub>2</sub>: optimization of process conditions through sequential Doehlert design

Isadora L. C. Cunha<sup>1</sup> · Antonio Carlos S. C. Teixeira<sup>1</sup>

Received: 29 July 2020 / Accepted: 8 March 2021 / Published online: 16 March 2021  
© The Author(s), under exclusive licence to Springer-Verlag GmbH Germany, part of Springer Nature 2021

## Abstract

The degradation of three pesticides, azoxystrobin (AZO), difenoconazole (DFZ), and imidacloprid (IMD), commonly found in the tomato rinse water, was studied through UVC (251–257 nm) and UVC/H<sub>2</sub>O<sub>2</sub> photolysis. The results showed that direct photolysis follows pseudo-first-order kinetics, with total AZO and IMD removals within 15 min, using 21.8 and 28.6 W m<sup>-2</sup>, respectively, while the highest percentage of DFZ degradation was 51.7% at 28.6 W m<sup>-2</sup> UVC. The estimated quantum yields were 0.572, 0.028, and 0.061 mol Einstein<sup>-1</sup> for AZO, DFZ, and IMD, respectively. With regard to UVC/H<sub>2</sub>O<sub>2</sub>, total pesticide removal was achieved after 10 min, while optimal treatment conditions in relation to the pesticide removal rates, estimated through the sequential Doehlert design, were about [H<sub>2</sub>O<sub>2</sub>]<sub>0</sub> = 130 mg L<sup>-1</sup> and 26 W m<sup>-2</sup>. Cytotoxicity and genotoxicity assays carried out with *Allium cepa*, for real industrial tomato rinse water sampled from washing belts did not show abnormalities during cell division, with total pesticides degradation after 15 min, demonstrating the potential application of the UVC/H<sub>2</sub>O<sub>2</sub> process as a viable localized treatment with a focus on the possible reuse of treated water.

**Keywords** Advanced oxidation processes · Azoxystrobin · Imidacloprid · Difenoconazole · Doehlert design · Cytotoxicity · Genotoxicity

## Introduction

In recent years, the population's demand for quality food has increased and, as a result, pesticides have been increasingly used for pest control in fruits and vegetable cultivations. Currently, Brazil is one of the largest agricultural producers in the world and since 2008, the largest pesticide consumer, having used around 540,000 tons of active ingredients in 2017 alone (Bombardi 2017). Also, the number of new commercial products registered has been growing every year, with 211 recorded until June 2020 (MAPA 2020).

Among these compounds, imidacloprid (IMD) is an efficient systemic insecticide against sucking insects, acting directly on their central nervous system (Fenoll et al. 2015). Azoxystrobin (AZO) is a systemic fungicide of the strobilurine family, effective against a wide range of fungal diseases (Calza et al. 2006). Difenoconazole (DFZ) is a fungicide used for prevention and cure for several cultures, capable of interfering with the growth of fungi and inhibiting spore germination (Li et al. 2013). These compounds are constituents of several commercial products handled in Brazilian cultivations, including tomato and raw material for several products in the agroindustry. Their respective structural formulas are given in Fig. 1.

In line with the good agricultural practices established by legislation, a certain period before harvesting should be respected after agrochemicals application, so that the compounds can act properly in pest control, and food residues can be reduced. Studies such as those by Andrade et al. (2015) and Rodrigues et al. (2017) have shown that, even though this period is respected, a fraction of the compounds

Responsible Editor: Ricardo Torres-Palma

✉ Isadora L. C. Cunha  
isadoracunha@usp.br

<sup>1</sup> Research Group in Advanced Oxidation Processes (AdOx), Department of Chemical Engineering, Escola Politécnica, University of São Paulo, Av. Prof. Luciano Gualberto, 380, CEP 05508-010 São Paulo, SP, Brazil

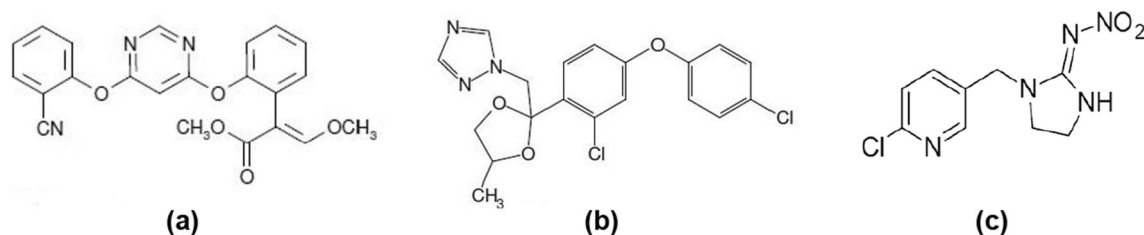


**Fig. 1** Structural formulas of **a** azoxystrobin-AZO [methyl (E)-2-[2-[6-(2-cyanophenoxy)pyrimidin-4-yl]oxyphenyl]-3-methoxyprop-2-enoate,  $C_{22}H_{17}N_3O_5$ , CAS 131860-33-8]; **b** difenoconazole-DFZ [1-((2-(2-chloro-4-(4-chlorophenoxy)phenyl)-4-methyl-1,3-dioxolan-2-

yl)methyl)-1H-1,2,4-triazole,  $C_{19}H_{17}Cl_2N_3O_3$ , CAS 119446-68-3]; and **c** imidacloprid-IMD [(NE)-N-[1-[(6-chloropyridin-3-yl)methyl]imidazolidin-2-ylidene]nitramide,  $C_9H_{10}ClN_5O_2$ , CAS 138261-41-3]

that were not absorbed is transferred to water during fruit and vegetable washing before final processing. However, even at low concentrations, these contaminants can cause adverse effects on human health and on the environment. Silva et al. (2016) reported that the continuous exposure of bees to IMD concentrations of 4.25 and 21.25  $\text{ng } \mu\text{L}^{-1}$  alters their locomotion ability, which may affect their search for food and compromise hives. In addition, Han et al. (2016) verified the harmful effect of AZO upon aquatic organisms, while Pan et al. (2017) observed that DFZ can act as an endocrine disruptor.

According to Maurya et al. (2019), triazole fungicides, such as DFZ, have high photochemical stability and low biodegradability. Monsalvo et al. (2014) investigated the biodegradability and toxicity of three pesticides, among which IMD, in an expanded granular sludge bed reactor, finding that IMD was not removed after more than 20 days, while Tişler et al. (2009) found that IMD was not rapidly biodegraded in aquatic environments. However, specific studies on AZO biodegradability have not been found in the literature. As a consequence, since conventional effluent treatment processes are not able to completely remove these compounds, advanced oxidation processes (AOP) have gained prominence as alternative treatment strategies. These processes are efficient in removing persistent organic compounds through the action of hydroxyl radicals ( $\text{HO}\cdot$ ), which can react with pollutants and practically achieve their complete degradation (Bethi et al. 2016; Ameta 2018).

With regard to wastewater treatment containing pesticides, the literature reports studies related to IMD degradation by AOPs, such as photo-Fenton (Segura et al. 2008), photocatalysis (Rózsa et al. 2019; Kanwal et al. 2018), and ozonation (Baghirzade et al. 2020) since this compound has recently been included in the European List of Priority Substances through Decision 2015/495/EU (Barbosa et al. 2016). Zapata et al. (2010) investigated combined solar photocatalysis and biological treatments, applied to IMD degradation, while at high concentrations ( $43 \text{ mg L}^{-1}$ ). As for AZO and DFZ, these compounds were detected in water sources in Brazil (Caldas et al. 2013). However, there is a lack of studies investigating AOPs for degrading these

compounds; some involving photo-Fenton, photo-Fenton like, and photocatalysis have been found in the literature (Bessergenev et al. 2017; Aliste et al. 2020; Garrido et al. 2020) but none concerning  $\text{UVC}/\text{H}_2\text{O}_2$  or with the three target contaminants in the mixture.

The  $\text{UVC}/\text{H}_2\text{O}_2$  process consists in the generation of  $\text{HO}\cdot$  radicals through O–O bond breakdown of hydrogen peroxide molecules by ultraviolet (UVC) radiation (Mierzwa et al. 2018). In comparison with other AOPs, the following advantages of this process can be mentioned (Tang 2004): (i) organic pollutants can be degraded either by photolysis or by hydroxyl radicals; (ii) microorganisms present in the medium can be inactivated by UVC radiation, while hydroxyl radicals are effectively generated (Mierzwa et al. 2018); (iii) high  $\text{H}_2\text{O}_2$  water solubility allowing the storage of its solutions and facilitating their handling and mixing with the effluent to be treated, in contrast to ozonation, in which the transfer of the gaseous oxidant to the aqueous phase is subject to mass transfer limitations; (iv) there is no generation of sludge (as is the case of Fenton and photo-Fenton) or air emissions; (v) no further processing, separation (as is the case of  $\text{TiO}_2$  photocatalysis), or disposal is required; (v) simple operation and implantation.

Miklos et al. (2018) classified the  $\text{UVC}/\text{H}_2\text{O}_2$  process as energetically viable, together with ozonation,  $\text{O}_3/\text{H}_2\text{O}$ ,  $\text{O}_3/\text{UVC}$ , UV/persulfate, and UV/chlorine, based on the reported values for the parameter *electric energy per order of magnitude* ( $E_{\text{EO}}$ ). This parameter represents the amount of electric energy in kilowatt-hour necessary to degrade a contaminant by one order of magnitude in  $1 \text{ m}^3$  of contaminated water, normally associated with the largest portion of operating costs (Bolton et al. 2001). The aforementioned processes present median values of  $E_{\text{EO}} < 1 \text{ kWh m}^{-3} \text{ order}^{-1}$ , thus presenting the potential for industrial application, unlike photo-Fenton, plasma, and electrolytic AOPs (median values of  $E_{\text{EO}} = 1\text{--}100 \text{ kWh m}^{-3} \text{ order}^{-1}$ ), of high energetic cost, but which can represent attractive solutions depending on the application, and UV-based photocatalysis, ultrasound, and microwave-based processes (median values of  $E_{\text{EO}} > 100 \text{ kWh m}^{-3} \text{ order}^{-1}$ ), not considered energy-efficient AOPs so far (Miklos et al. 2018). Moreover, Fast et al. (2017) carried

out a comparative study of advanced oxidative processes in the removal of contaminants of emerging concern based on environmental, engineering, social, and economic aspects. According to the proposed classification, with scores varying from 1 to 5, the UVC/H<sub>2</sub>O<sub>2</sub> process had an overall score of 3.36, being therefore advantageous in comparison with ozonation, UVC/O<sub>3</sub>, Fenton, and TiO<sub>2</sub>-based photocatalysis (scores 3.30, 3.08, 2.89, and 2.11, respectively), especially with regard to the criteria of acceptance and ease of application. In fact, according to the authors, the UVC/H<sub>2</sub>O<sub>2</sub> process is a well-established technology, with low energy consumption and low impacts on climate change. In any case, as remarked by Katsoyiannis et al. (2011), the energy demand of the UVC/H<sub>2</sub>O<sub>2</sub> process strongly depends on parameters such as hydrogen peroxide concentration, optical path length, nature of the target pollutant, and complexity of the aqueous matrix to be treated.

This study thus aimed at evaluating the degradation of the active ingredients AZO, DFZ, and IMD, commonly used in Brazilian cultivations and found in the rinse water generated in tomato processing in the agroindustry. The pesticides were used at typical wastewater concentrations, and the efficiency of direct photolysis and UVC/H<sub>2</sub>O<sub>2</sub> on their degradation was investigated by evaluating the effects of process variables (initial hydrogen peroxide concentration, [H<sub>2</sub>O<sub>2</sub>]<sub>0</sub>; 254-UVC irradiance,  $E_{\text{UVC}}$ ) through sequential experimental design based on the Doehlert matrix. Furthermore, additional experiments were carried out using real rinse water sampled in the industry, for which cytotoxicity and genotoxicity were investigated, based on the test organism *Allium cepa*.

## Materials and methods

### Reagents

The commercial products Amistar Top® (Syngenta), containing in its formulation the active ingredients AZO and DFZ, and Provado 200 SC® (Bayer), containing the active ingredient IMD, were used in all the experiments. For the UVC/H<sub>2</sub>O<sub>2</sub> assays, a 30% (w/w) hydrogen peroxide solution (Labsynth) was used. Acetonitrile (HPLC grade), purchased from Sigma Aldrich, and ultrapure water were used in HPLC procedures. HCl was obtained from Vetec. AZO, DFZ, and IMD analytical standards (Sigma Aldrich) were used for determining the molar absorption coefficients ( $\epsilon$ ). All the solutions were prepared in Milli-Q® water, produced in a Milli-Q® Direct-Q system (Merck Millipore) (18.2 M $\Omega$  cm).

### Molar absorption coefficients ( $\epsilon$ )

In order to obtain the molar (decadic) absorption coefficients ( $\epsilon_{\lambda}$ ) of the pesticides, pure stock solutions (80 mg L<sup>-1</sup>) were prepared by dissolving the analytical standard of each active compound in

Milli-Q® water at room temperature. In the sequence, the stock solutions were diluted to 0.8, 1.2, 1.6, 2.0, and 4.0 mg L<sup>-1</sup> (i.e., 1.98–9.92  $\mu\text{mol L}^{-1}$  AZO; and 1.97–9.85  $\mu\text{mol L}^{-1}$  DFZ) and to 0.63, 0.99, 1.27, 1.64, and 3.35 mg L<sup>-1</sup> (2.46–13.1  $\mu\text{mol L}^{-1}$  IMD). The decadic absorbance ( $A_{10}$ ) of each solution at a given molar concentration  $c$  was then measured as a function of wavelength in the range 190–800 nm using a UV/VIS Varian Cary 50 spectrophotometer and a 1-cm path length quartz cuvette. The values of  $\epsilon_{\lambda}$  were then obtained for each pesticide and wavelength from the slope of the straight line on a graph of  $A_{10,\lambda} \times$  (Skoog et al. 2017).

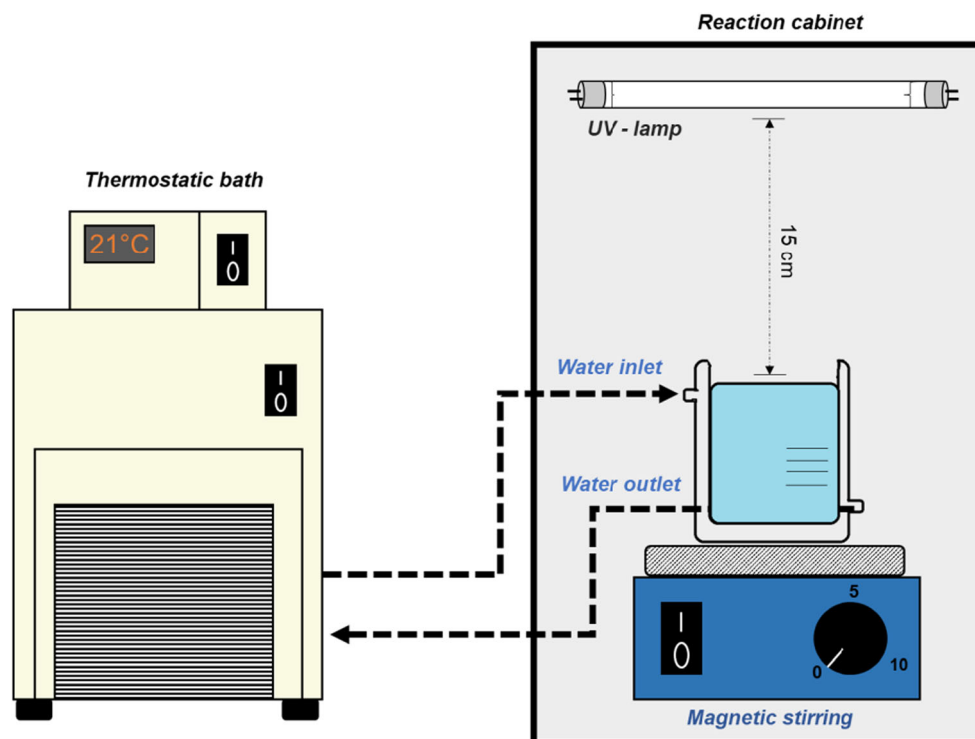
### Synthetic tomato rinse water

Concentrated aqueous solutions of the commercial products Amistar Top® and Provado 200 SC® were first prepared according to the manufacturer's specifications for tomato cultivation. Then, based on information provided by the State Technical Assistance and Rural Extension Company of Minas Gerais (EMATER-MG, Brazil), regarding the average yield of tomato plants per hectare (~ 80,000-kg tomatoes per hectare) and the manufacturers' recommendations that 1000 L of syrup is applied per hectare, it was found that about 0.0125 L of pesticides syrup is sprayed per each kilogram of tomatoes. In addition, knowing that washing operations in the industry are usually repeated ten times before fruit processing, using a proportion of about 3 L of water per kilogram of tomatoes, the concentrations of each active ingredient in the rinse water could be obtained, assuming that the pesticides are retained in tomatoes surface and completely removed during washing. Therefore, the concentrated solutions were diluted in order to obtain the nominal concentrations 3.0, 2.0, and 3.0 mg L<sup>-1</sup> of AZO, DFZ, and IMD, respectively. The resulting solution, therein referred to as synthetic rinse water, containing the three active ingredients, was used in the degradation experiments. The calculations are detailed in the Supplementary Material.

### Photochemical reactor

Degradation experiments were conducted in a benchtop photochemical reactor, placed inside a closed reaction cabinet, and equipped with UVC lamps (Philips TUV 8W/G8TS) emitting at in the wavelength range 251–257 nm ( $\lambda_{\text{max}} = 254$  nm). Irradiances were measured using a spectroradiometer (Luzchem, SPR-4002), at 15 cm away from the lamps, giving  $E_{\text{UVC}} = 15.0, 21.8, \text{ and } 28.6 \text{ W m}^{-2}$ , for 2, 3, and 4 lamps, respectively. A 250-mL capacity jacketed beaker was filled with 150 mL of synthetic rinse water; the liquid surface was placed 15 cm away from the lamps, and a thermostatic bath was used to maintain its temperature at 21 °C. The solution was continuously stirred to keep homogeneity. Figure 2 presents a scheme of the experimental apparatus.

**Fig. 2** Scheme of the experimental apparatus



### Photodegradation experiments using synthetic rinse water: direct photolysis and UVC/H<sub>2</sub>O<sub>2</sub>

For photolytic experiments in the absence of H<sub>2</sub>O<sub>2</sub>, 150 mL of the synthetic rinse water containing the three active ingredients (AZO, IMD, and DFZ) was placed in the photochemical reactor and irradiated at 15.0, 21.8, and 28.6 W m<sup>-2</sup> for 15 min. One-mL aliquots were withdrawn at 0, 0.25, 0.50, 0.75, 1, 2, 5, 10, and 15 min, and analyzed by HPLC.

In the case of UVC/H<sub>2</sub>O<sub>2</sub>, the experiments were carried out for 15 min, using 150 mL of the synthetic rinse water containing the three active ingredients (AZO, IMD, and DFZ), varying the initial H<sub>2</sub>O<sub>2</sub> concentrations and UVC irradiances. The amount of 30% (w/w) hydrogen peroxide solution was added at time zero to obtain the desired value of [H<sub>2</sub>O<sub>2</sub>]<sub>0</sub>. One-mL aliquots were withdrawn at 0, 0.25, 0.50, 0.75, 1, 2, 5, 10, and 15 min; diluted with 100 μL methanol to quench the reaction, according to the methodology of Lastre-Acosta et al. (2019); and analyzed by HPLC. The experiments were conducted following sequential Doehlert experimental designs, combined with response surface analysis, aiming to explore the effects of the initial H<sub>2</sub>O<sub>2</sub> concentration and irradiance on active ingredients degradation and to obtain the best experimental condition in terms of the highest pseudo-first-order specific degradation rate of each compound. This experimental design approach was first proposed by Doehlert in 1970 (Novaes et al. 2017) and has the following advantages: low number of experiments required to reach the optimal result, hence requiring less reagents and time; spherical experimental

domain, with uniformity in space filling; easy extension of the experimental domain by adding another factor or displacing the design, making it possible to use data from previous experiments (Sena et al. 2012; Caldas et al. 2012).

In this work, a Doehlert matrix with two variables was used, with  $x_1$  equivalent to the initial H<sub>2</sub>O<sub>2</sub> concentration and  $x_2$  to the irradiance. Table 1 shows the conditions of the base design (runs 1–9, Fig. 3), comprising seven runs plus two replicates at the central point conditions, with [H<sub>2</sub>O<sub>2</sub>]<sub>0</sub> varying in the range 24.9–99.5 mg L<sup>-1</sup>, corresponding to 1–4 times the stoichiometric amount needed to achieve the complete mineralization of the active ingredients present in the synthetic rinse water. The values of  $E_{UVC}$  were set in the range 15.0–28.6 W m<sup>-2</sup> (2–4 Philips TUV 8W/G8TS UVC lamps).

In order to explore the effect of [H<sub>2</sub>O<sub>2</sub>]<sub>0</sub> on pesticide degradation, the design was then moved across the  $x_1$  axis in the experimental domain, for both higher and lower oxidant dosages. For this purpose, three additional experiments (runs 10–12) were first added. Subsequently, a second experimental matrix was built (runs 13–18), with [H<sub>2</sub>O<sub>2</sub>]<sub>0</sub> ranging from 12.4 to 37.3 mg L<sup>-1</sup>, i.e., 0.5 to 1.5 times the calculated stoichiometric ratio (Fig. 3). In any case, Table 1 presents the coded and real values of the independent variables used in the UVC/H<sub>2</sub>O<sub>2</sub> experiments;  $x_i$  and  $C_i$  are related by Eq. (1), where  $C_i$  and  $x_i$  correspond to the coded and real values of variable  $i$ , respectively;  $x_i^0$  refers to the conditions of the central point of the base design,  $\Delta x_i$  is the step of variation, and  $\alpha$  is the coded value limit of each variable (Ferreira et al. 2004).

**Table 1** Experimental conditions used in the UVC/H<sub>2</sub>O<sub>2</sub> experiments and values of the pseudo-first-order specific degradation rates for each pesticide

| Run | Coded values   |                | Experimental values  |  |
|-----|----------------|----------------|--|--|
|     | C <sub>1</sub> | C <sub>2</sub> | x <sub>1</sub> , [H <sub>2</sub> O <sub>2</sub> ] <sub>0</sub> (mg L <sup>-1</sup> ) | x <sub>2</sub> , irradiance (E <sub>UVC</sub> ) (W m <sup>-2</sup> ) |
| 1   | 0              | 0              | 62.2   | 21.8   |
| 2   | 0              | 0              | 62.2   | 21.8   |
| 3   | 0              | 0              | 62.2   | 21.8   |
| 4   | 1.0            | 0              | 99.5   | 21.8   |
| 5   | 0.500          | 0.866          | 80.9   | 28.6   |
| 6   | -1.0           | 0              | 24.9   | 21.8   |
| 7   | -0.500         | -0.866         | 43.5   | 15.0   |
| 8   | 0.500          | -0.866         | 80.9   | 15.0   |
| 9   | -0.500         | 0.866          | 43.5   | 28.6   |
| 10  | 1.500          | 0.866          | 118.2  | 28.6   |
| 11  | 1.500          | -0.866         | 118.2  | 15.0   |
| 12  | 2.0            | 0              | 136.8  | 21.8   |
| 13  | -0.667         | 0              | 37.3   | 21.8   |
| 14  | -0.833         | 0.866          | 31.1   | 28.6   |
| 15  | -1.333         | 0              | 12.4   | 21.8   |
| 16  | -1.167         | -0.866         | 18.7   | 15.0   |
| 17  | -0.833         | -0.866         | 31.1   | 15.0   |
| 18  | -1.167         | 0.866          | 18.7   | 28.6   |

$$C_i = \left\{ \frac{x_i - x_i^0}{\Delta x_i} \right\} \alpha \tag{1}$$

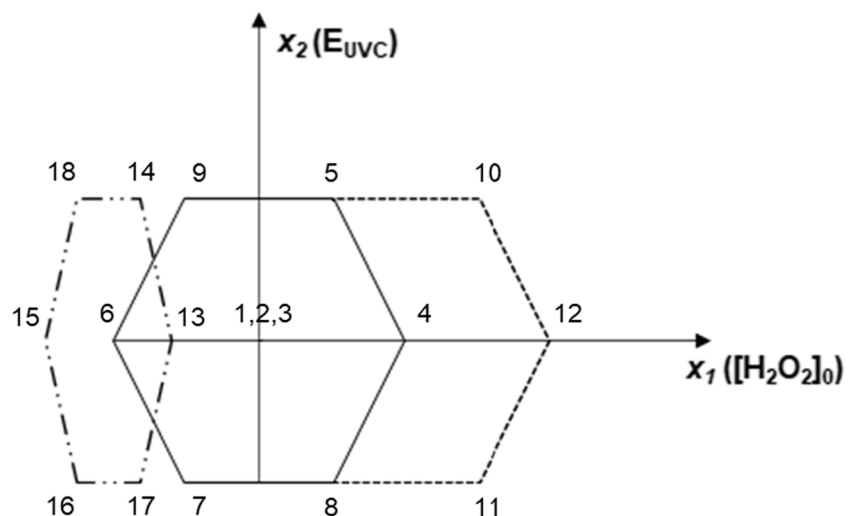
STATGRAPHICS Plus®, 5.0 Version (Statgraphics Technologies Inc.) was used for data analysis and response surface calculations.

### Treatment of real rinse water by UVC/H<sub>2</sub>O<sub>2</sub>

In order to evaluate the performance of the UVC/H<sub>2</sub>O<sub>2</sub> process with real aqueous matrices, samples of tomato rinse water were collected at two points in the industry (Figure S1): (i) during the unloading of truck bodies containing freshly harvested fruits, which is done with the aid of water jets (*pre-*

*washing*) and (ii) in the final washing stage carried out on conveyor belts, immediately before the selection of fruits for processing intended for the manufacture of food products (*washing belts*). Some characteristics of these water samples are presented in Table S1. The samples were stored at -4 °C until used in the experiments. For that, the rinse water samples were spiked with the commercial products Amistar Top® and Provado 200 SC® to obtain the working nominal pesticides concentrations (3.0, 2.0, and 3.0 mg L<sup>-1</sup> for AZO, DFZ, and IMD, respectively). One-mL aliquots were withdrawn during irradiation in the presence of hydrogen peroxide at 0, 0.25, 0.50, 0.75, 1.0, 2.0, 5.0, 10.0, and 15.0 min, diluted with 100 µL methanol, filtered using 0.45-µm PVDF membranes, and analyzed by HPLC.

**Fig. 3** Doehlert matrices used in the UVC/H<sub>2</sub>O<sub>2</sub> experiments



## Analytical methods

Active ingredients concentrations were followed over time using a Shimadzu ultra-fast liquid chromatograph (UFLC, LC 20AD), equipped with a UV/VIS detector (SPD 20A) and a C18 column (250 × 4.60 mm, 5- $\mu$ m particle size). Based on the methods developed by Al-Rimawi (2016), Yaqub et al. (2017), and Tsochatzis et al. (2011), the mobile phase at 1.0 mL min<sup>-1</sup> consisted of Milli-Q® water (A) and acetonitrile (B); elution followed the gradient: 50% B (0–3 min); increase to 80% B (3–12 min); 80% B (12–14 min); decrease from 80 to 50% B (14–18 min). The oven temperature was maintained at 40 °C and the injection volume was 100  $\mu$ L. AZO and DFZ were determined at 254 nm and IMD at 270 nm. A calibration curve was obtained for each pesticide; the values of the determination coefficient ( $R^2$ ), limit of detection (LOD, mg L<sup>-1</sup>), and limit of quantification (LOQ, mg L<sup>-1</sup>) obtained are, respectively 0.996, 1.282, and 2.564 (AZO); 0.988, 0.355, and 1.077 (DFZ); and 1.000, 0.122, and 0.244 (IMD). The values of LOD and LOQ were estimated according to Ribani et al. (2004).

## Cytotoxicity and genotoxicity assays

For the study of cytotoxicity and genotoxicity, experiments were carried out using tomato rinse water sampled in the industry (from pre-washing and washing belts, Figure S1 and Table S1), spiked with the commercial products Amistar Top® and Provado 200 SC®, and submitted to the UVC/H<sub>2</sub>O<sub>2</sub> treatment at the optimum conditions of [H<sub>2</sub>O<sub>2</sub>]<sub>0</sub> and  $E_{UVC}$  indicated by the Doehlert design. The tests were carried out using *Allium cepa*, according to the methodology proposed by Fiskesjö (1985). For this purpose, onion bulbs purchased in a local market were placed in water to germinate for 72 h, without direct sunlight. After the roots grew, they were exposed in duplicate to tap water (negative control), as well as to treated and untreated rinse water, for 48 h, at room temperature. The roots were then collected and subjected to hydrolysis with 1.0-mol L<sup>-1</sup> HCl solution at 60 °C for 10 min. Slides were then prepared with root meristem cells, which were stained using the Panótico Rápido® kit (Laborclin) in all cell colorations, and observed under an optical microscope (Zeiss Axio Scope A1). Qualitatively, genotoxic effects are associated with changes such as micronuclei, binucleate cells, and nuclear buds, while the cytotoxic effects are quantified through the analysis of mitotic changes, considering the phases of cell division (prophase, metaphase, anaphase, and telophase). The mitotic index (MI) was calculated as the ratio between the number of cells observed in any of the division phases (NDC) and the total number of cells analyzed (NTC) (with a count of up to 100 cells), according to Eq. (2):

$$MI(\%) = \frac{NDC}{NTC} \times 100 \quad (2)$$

## Results and discussion

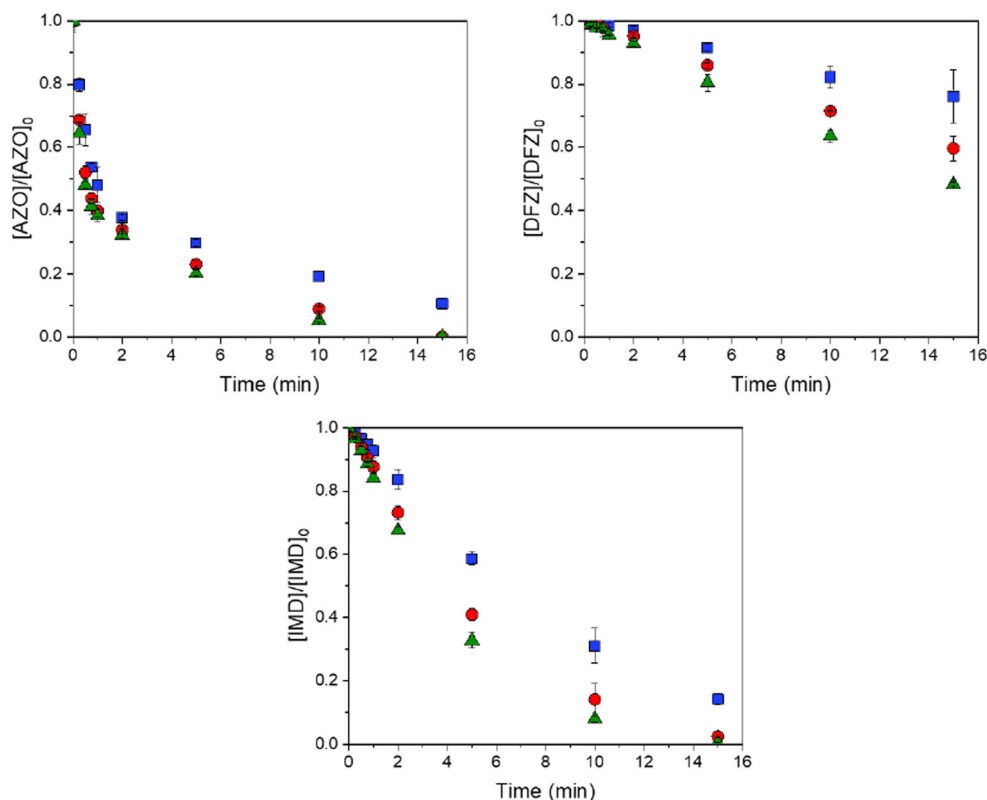
### Direct photolysis

The highly energetic electronically excited state of a contaminant molecule, reached by UV radiation absorption, deactivates very rapidly to the lowest excited state (Oppenländer 2003), which then deactivates to the ground state through radiative (fluorescence, phosphorescence) and non-radiative physical processes (Parsons 2005). The lowest electronic excited states of contaminant molecules may also undergo chemical reactions through hemolytic bond scission in the solvent cage, forming carbon-centered radicals (R•); however, the likelihood of radical recombination is high, explaining the usual low photolysis quantum yields and thus limiting the industrial application of direct photolysis. Despite that, carbon-centered radicals may escape from the solvent cage and react with dissolved oxygen, giving peroxy (RO<sub>2</sub>•) and oxy (RO•) radicals, generating further photoproducts. Intramolecular electron transfer, resulting in heterolytic bond scissions, may also occur in water. In addition, triplet excited states of organic pollutants may interact with dissolved oxygen through energy and electron transfer processes, resulting in contaminant molecules in the ground state and singlet oxygen, and contaminant radical cations and superoxide radical anions (O<sub>2</sub>•<sup>-</sup>), respectively (Oppenländer 2003; Parsons 2005).

The results of AZO, DFZ, and IMD degradation by direct photolysis are shown in Fig. 4.

A sharp decrease in AZO concentration occurred for short irradiation times, under all irradiation conditions. Direct photolysis using 15.0 W m<sup>-2</sup> achieved 89.4% pesticide removal within 15 min, with AZO concentrations below the detection limit for 21.8 and 28.6 W m<sup>-2</sup>. DFZ showed to be more persistent and not completely degraded by direct photolysis (maximum 51.7% removal after 15 min for  $E_{UVC} = 28.6$  W m<sup>-2</sup>). The pseudo-first-order specific photolysis rates ( $k'$ ) increased with increasing irradiance for the three pesticides, varying in the ranges 0.128–0.249 s<sup>-1</sup> (AZO), 0.019–0.048 s<sup>-1</sup> (DFZ), and 0.129–0.266 s<sup>-1</sup> (IMD) (Fig. 5 and Table S2); the corresponding determination coefficients were satisfactorily high, with  $R^2 = 0.895$ –0.928, 0.986–0.997, and 0.981–0.995 for AZO, DFZ, and IMD, respectively (Table S2). The direct photolysis quantum yields of AZO, DFZ, and IMD were calculated from the concentration-time data, knowing the absorptivity of each compound in the UVC and the irradiance in each case.

**Fig. 4** AZO, DFZ, and IMD decay over time by direct photolysis, for  $E_{UVC} = 15.0 \text{ W m}^{-2}$  (blue square),  $21.8 \text{ W m}^{-2}$  (red circle), and  $28.6 \text{ W m}^{-2}$  (green triangle). Experiments were performed with synthetic rinse water containing the three pesticides:  $[\text{AZO}]_0 = 2.83 \pm 0.06 \text{ mg L}^{-1}$ ;  $[\text{DFZ}]_0 = 1.54 \pm 0.03 \text{ mg L}^{-1}$ ;  $[\text{IMD}]_0 = 2.74 \pm 0.01 \text{ mg L}^{-1}$ . The average errors are 1.8% (AZO), 1.1% (DFZ), and 2.8% (IMD)



The absorption of UV-vis radiation by a compound at a given wavelength is proportional to the product of its molar absorption coefficient ( $\epsilon$ ) and molar concentration,  $c$  ( $\text{mol L}^{-1}$ ). On the other hand, according to Braun et al. (1991), the quantum yield  $\Phi$  of a photochemical reaction corresponds to the number of moles of reactant consumed or product formed, in a given time interval, divided by the number of moles of photons (i.e., Einstein) absorbed by the reactant over the same time. The rate at which a photochemical reaction occurs following irradiation depends on the overlap of the absorption and activation spectra (curves  $\epsilon_\lambda$  and  $\Phi_\lambda$ , respectively) of the compound under consideration within a given wavelength range. Given these considerations, for the UVC radiation emitted by the lamps (251–257 nm,  $\lambda_{\text{max}} = 254 \text{ nm}$ ), comparing AZO ( $\epsilon_{\text{AZO}} = 1572 \text{ L mol}^{-1} \text{ cm}^{-1}$ ) and DFZ ( $\epsilon_{\text{DFZ}} = 1701 \text{ L mol}^{-1} \text{ cm}^{-1}$ ) (Figure S2), the lower specific photolysis rate of DFZ can therefore be attributed to its lower value of  $\epsilon \times c$  at time zero ( $0.011$  and  $0.006 \text{ cm}^{-1}$  for AZO and DFZ, respectively) and to its low photolysis quantum yield ( $\Phi_{\text{DFZ}} = 0.028 \text{ mol Einstein}^{-1}$ ). In the case of IMD, even though this compound has the highest molar absorption coefficient at 254 nm among the three pesticides ( $\epsilon_{\text{IMD}} = 12817 \text{ L mol}^{-1} \text{ cm}^{-1}$ , see Figure S2), and the highest initial  $\epsilon \times c$  ( $0.135 \text{ cm}^{-1}$ ), its estimated photolysis quantum yield was consistently low ( $\Phi_{\text{IMD}} = 0.061 \text{ mol Einstein}^{-1}$ ). Therefore, the values of  $k'_{\text{IMD}}$  are higher than those of  $k'_{\text{DFZ}}$  but similar to the values of  $k'_{\text{AZO}}$ . The highest photolysis quantum yield in the

wavelength range 251–257 nm was obtained for AZO ( $\Phi_{\text{AZO}} = 0.572 \text{ mol Einstein}^{-1}$ ), which is one order of magnitude higher than those found for DFZ and IMD.

Boudina et al. (2007) suggested that the phototransformation of AZO in aqueous solution at wavelengths  $> 290 \text{ nm}$  involves multiple, parallel reaction pathways, including photo-isomerization; photo-hydrolysis of the methyl ester and of the nitrile group; cleavage of the acrylate double bond; photohydrolytic ether cleavage between the aromatic ring, giving phenol; and oxidative cleavage of the acrylate double bond. Zheng et al. (2004) studied the direct and sensitized photolysis of aqueous IMD at 254 nm, observing the formation of  $\text{CO}_2$ ,  $\text{Cl}^-$ , and  $\text{NO}_3^-$ , the latter occurring by the formation of  $\text{NH}_4^+$  and  $\text{NO}_2^-$ . In turn, according to Todey et al. (2018), the urea derivative was identified as the most common product formed from the hydrolysis and photolysis of neonicotinoid insecticides, among which IMD.

### UVC/H<sub>2</sub>O<sub>2</sub> process

The influence of irradiance and  $[\text{H}_2\text{O}_2]_0$  on AZO, DFZ, and IMD degradation was investigated through the nine preliminary experiments of the base Doehlert design (Table 1 and Fig. 3). In comparison with direct photolysis, complete pesticide removal was achieved, with concentrations falling below the detection limit in the first ten min of irradiation for most conditions (Figures S3–S8). As expected, pesticides

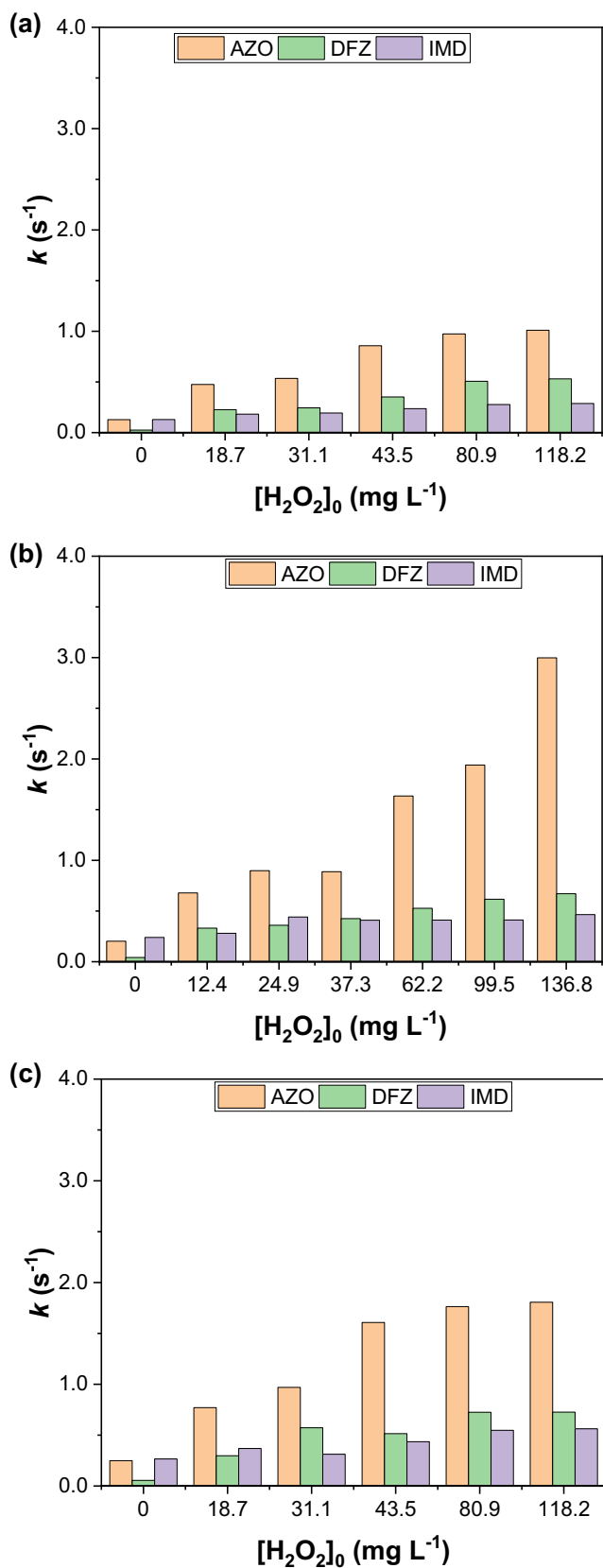


**Fig. 5** Pseudo-first-order specific degradation rates for the UVC/ $\text{H}_2\text{O}_2$  experiments of the Doehlert experimental design, carried out with different initial hydrogen peroxide concentrations and irradiances. **a**  $E_{UVC} = 15 \text{ W m}^{-2}$ ; **b**  $E_{UVC} = 21.8 \text{ W m}^{-2}$ ; and **c**  $E_{UVC} = 28.6 \text{ W m}^{-2}$

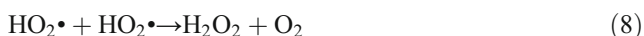
degradation occurred faster for higher oxidant concentration (at fixed  $E_{UVC}$ ) and irradiance (at fixed  $[\text{H}_2\text{O}_2]_0$ ), as confirmed by the pseudo-first-order specific degradation rates  $k_{\text{AZO}}$ ,  $k_{\text{DFZ}}$ , and  $k_{\text{IMD}}$ , which varied in the ranges  $0.475\text{--}2.998 \text{ s}^{-1}$ ,  $0.226\text{--}0.726 \text{ s}^{-1}$ , and  $0.182\text{--}0.562 \text{ s}^{-1}$ , respectively (Fig. 5 and Table S3). The determination coefficients ( $R^2$ ) for the  $k$ -values varied in the range  $0.871\text{--}0.998$  (AZO),  $0.965\text{--}0.998$  (DFZ), and  $0.963\text{--}0.999$  (IMD) (Table S3), while the experimental error, estimated from the three replicates in the conditions of the central point (runs 1–3) was 3.0% (AZO), 2.2% (DFZ), and 2.5% (IMD).

The  $k$ -values were consistently much higher for AZO, for both the photolytic and UVC/ $\text{H}_2\text{O}_2$  processes, and all irradiances studied (Fig. 5 and Table S3). In addition,  $k_{\text{AZO}}$  increased steadily with increasing initial hydrogen peroxide concentration, achieving almost constant values of about  $1.0 \text{ s}^{-1}$  ( $[\text{H}_2\text{O}_2]_0 = 80.9 \text{ mg L}^{-1}$ ,  $E_{UVC} = 15 \text{ W m}^{-2}$ ),  $1.9 \text{ s}^{-1}$  ( $[\text{H}_2\text{O}_2]_0 = 99.5 \text{ mg L}^{-1}$ ,  $E_{UVC} = 21.8 \text{ W m}^{-2}$ ), and  $1.8 \text{ s}^{-1}$  ( $[\text{H}_2\text{O}_2]_0 = 80.9 \text{ mg L}^{-1}$ ,  $E_{UVC} = 28.6 \text{ W m}^{-2}$ ); for  $E_{UVC} = 21.8 \text{ W m}^{-2}$ , a further increase in  $[\text{H}_2\text{O}_2]_0$  to  $136.8 \text{ mg L}^{-1}$  resulted in about 55% increase in  $k_{\text{AZO}}$ . In contrast, the values of  $k_{\text{DFZ}}$  and  $k_{\text{IMD}}$  were closer to each other, particularly for low  $[\text{H}_2\text{O}_2]_0$  and/or  $E_{UVC}$ ; the highest values found were about  $0.73 \text{ s}^{-1}$  and  $0.55 \text{ s}^{-1}$ , respectively, for  $[\text{H}_2\text{O}_2]_0 = 118.2 \text{ mg L}^{-1}$  and  $E_{UVC} = 28.6 \text{ W m}^{-2}$ . Finally, the results also suggest that the contribution of direct photolysis to the initial rate of pesticide degradation during the UVC/ $\text{H}_2\text{O}_2$  process followed the order  $\text{IMD} > \text{AZO} > \text{DFZ}$ . This is expected, given the competition between  $\text{H}_2\text{O}_2$  and pesticides molecules for incident photons, due to the much higher values of the molar absorption coefficients of the latter in comparison with that exhibited by  $\text{H}_2\text{O}_2$  in the same wavelength range (251–257 nm). In fact, if the effect of unknown absorbing intermediate compounds is neglected for simplification, the fraction of UVC radiation absorbed by the pesticides compared with hydrogen peroxide at time zero would be around 64–95% (IMD), 13–61% (AZO), and 7–46% (DFZ) (depending on  $[\text{H}_2\text{O}_2]_0$ ), clearly varying with time as both  $\text{H}_2\text{O}_2$  and pesticides concentrations decrease. Nevertheless, it is worth remarking that the role of the direct photolysis of each pesticide during the UVC/ $\text{H}_2\text{O}_2$  process, particularly for the lowest initial  $\text{H}_2\text{O}_2$  concentration levels, is intimately related to their particular UVC absorption properties and photolysis quantum yields.

The UVC-driven decomposition of hydrogen peroxide ( $\epsilon_{\text{H}_2\text{O}_2, 254 \text{ nm}} = 19 \text{ L mol}^{-1} \text{ cm}^{-1}$ , see Oppenländer 2003) follows the Haber-Weiss chain mechanism, according to which hydroxyl radicals formed by the photolytic cleavage of the O–O bond (Eq. (3),  $\Phi_{\text{HO}\cdot, 254 \text{ nm}} = 0.98 \text{ mol Einstein}^{-1}$ ) are scavenged by  $\text{H}_2\text{O}_2$  molecules, giving hydroperoxyl ( $\text{HO}_2\cdot$ ) radicals (Eq. (4)). These would form a six-membered cyclic complex ( $\text{HOO}\cdot\cdots\text{H}_2\text{O}_2$ ), which then rearranges by one-electron shifts to  $\text{H}_2\text{O}$ ,  $\text{O}_2$ , and  $\text{HO}\cdot$  (Eq.



(5)), the latter continuing the propagation cycle (Oppenländer 2003). The termination step of the chain mechanism involves radical-radical recombination reactions (Eqs. (6)–(8)). On the other hand, oxidation of target pesticides by HO• radicals mainly involves hydrogen abstraction and electrophilic addition to unsaturated bonds and aromatic systems (Oppenländer 2003), giving rise to carbon-centered organic radicals. The latter react immediately with dissolved O<sub>2</sub> to form peroxy radicals, which then undergo numerous molecular rearrangements and/or elimination reactions, leading to complex mixtures of oxidation products.



Some important information on the degradation of the target pesticides by AOPs is reported in the literature. Baghirzade et al. (2020) observed that IMD is resistant to degradation by O<sub>3</sub> but indirectly degraded by hydroxyl radicals, involving the loss of NO<sub>2</sub>, HNO<sub>2</sub>, and Cl<sup>-</sup>. Fiorenza et al. (2020) studied the use of photocatalysis, Fenton, and photo-Fenton in the degradation of IMD in water and found that its degradation is characterized by the formation of products such as amines and chloropyridine. In addition, according to the authors, the degradation mechanism of IMD involves the cleavage of the C–N and N–N bonds, followed by the formation of small molecules such as CO<sub>2</sub>, NO<sub>x</sub>, water, and ClO<sub>2</sub>. Navarro et al. (2011) investigated the removal of ten pesticides, including AZO, from leaching water in a pilot-scale plant by the sunlight-irradiated photo-Fenton treatment. In this study, hypotheses were raised regarding the reactions involving the hydroxyl radical and the target pesticides, through the abstraction of hydrogen from the C–H, N–H, or O–H bonds, and HO• addition to the double bond between carbon atoms or aromatic rings. Moreover, the authors comment on the presence of heteroatoms, which can result in the formation of inorganic acids. Since AZO contains nitrogen in its molecule, the authors argue that HNO<sub>3</sub> and NH<sub>4</sub><sup>+</sup> can be formed during degradation. Calza et al. (2006) verified the occurrence of concomitant AZO reaction pathways, in a study involving the transformation of different fungicides by TiO<sub>2</sub> photocatalysis. In this case, the AZO degradation pathways involved hydroxylation of the cyanophenyl ring, oxidation of the methyl groups, and breaking of the ether group between the cyanophenyl and pyrimidinyl rings. Finally, Pushkareva and Zenkevich (2018) studied the electrochemical oxidation

of DFZ and identified transformation products resulting from the substitution of chlorine of the aromatic ring and hydrogen atoms bonded to carbon atoms by hydroxyl groups or addition of oxygen to the molecule.

The corresponding analyses of variance (ANOVA) and Pareto charts indicate that for AZO and DFZ, only the linear effects of  $x_1$  ([H<sub>2</sub>O<sub>2</sub>]<sub>0</sub>) and  $x_2$  ( $E_{UVC}$ ) showed statistically positive significant values at the 95% confidence level (Tables S4 and S5; Figures S9 and S10, respectively), while for IMD, only the linear effect of  $E_{UVC}$  was significant (Table S6 and Figure S11). Therefore, although a fairly good fitting of the experimental data was obtained for AZO, DFZ, and IMD ( $R^2 = 0.782, 0.947, \text{ and } 0.815$ , respectively), the statistical analysis suggests that the base Doehlert design was not capable of identifying any quadratic effects of the independent variables within the experimental domain studied.

Therefore, additional experiments were included, varying the initial hydrogen peroxide concentration (Table 1 and Fig. 3). The results are shown in Table S3 and Fig. 5. Considering all the experiments performed, the ANOVA (Tables S7–S9) and the Pareto charts (Figures S12–S14) indicate the positive effects of both independent variables on the degradation rates of the three pesticides. For AZO and DFZ, [H<sub>2</sub>O<sub>2</sub>]<sub>0</sub> appears as the most influencing factor on  $k_{AZO}$  and  $k_{DFZ}$ , while irradiance showed to be more important regarding  $k_{IMD}$ . The negative value of the quadratic effect of  $E_{UVC}$  was statistically significant at the 95% confidence level for AZO and IMD, showing that the photooxidation rates of these pesticides increase with increasing irradiance, go through a maximum, and then stabilize. In contrast, for DFZ, the quadratic effect of the initial hydrogen peroxide concentration was statistically significant and negative, showing that  $k_{DFZ}$  increases with [H<sub>2</sub>O<sub>2</sub>]<sub>0</sub> and then decreases, suggesting the scavenging effect of radical species by the oxidant, an effect not observed for AZO and IMD. The corresponding response surface and contour plots (Fig. 6) confirm these trends for the three pesticides studied.

The statistical analysis using STATGRAPHICS Plus® enabled to obtain the quadratic response surface models for the dependent variables  $k_{AZO}$ ,  $k_{DFZ}$ , and  $k_{IMD}$  (Eqs. (9)–(11)) in terms of real independent variables, considering the significant factors only. The corresponding values of  $R^2$  were 0.827, 0.923, and 0.834, respectively, confirming the good fitting of the experimental data. From the quadratic models given by Eqs. (9)–(11), the optimum conditions were estimated as [H<sub>2</sub>O<sub>2</sub>]<sub>0</sub> = 136.8 mg L<sup>-1</sup> and  $E_{UVC}$  = 24.3 W m<sup>-2</sup> ( $k_{AZO}$  = 2.53 s<sup>-1</sup>); [H<sub>2</sub>O<sub>2</sub>]<sub>0</sub> = 127.3 mg L<sup>-1</sup> and  $E_{UVC}$  = 28.6 W m<sup>-2</sup> ( $k_{DFZ}$  = 0.75 s<sup>-1</sup>); and [H<sub>2</sub>O<sub>2</sub>]<sub>0</sub> = 136.8 mg L<sup>-1</sup> and  $E_{UVC}$  = 27.8 W m<sup>-2</sup> ( $k_{IMD}$  = 0.55 s<sup>-1</sup>).

$$k_{AZO} = -4.48949 + 0.01249x_1 + 0.43657x_2 - 0.00898x_2^2 \quad (9)$$

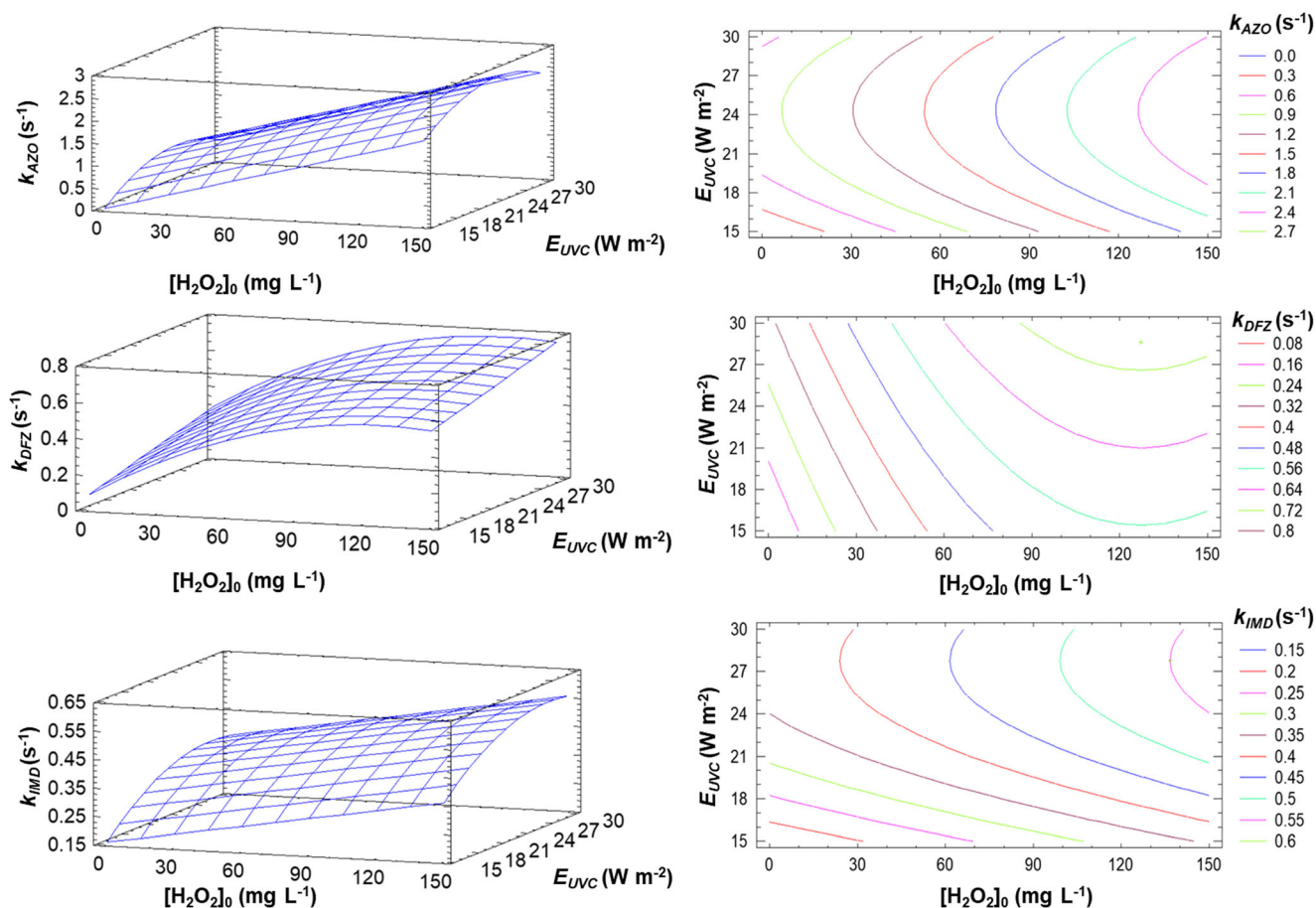


**Fig. 6** Response surfaces and contour plots for  $k_{\text{AZO}}$ ,  $k_{\text{DFZ}}$ , and  $k_{\text{IMD}}$  (UVC/ $\text{H}_2\text{O}_2$  process, runs (1)–(18)). Conditions:  $[\text{AZO}]_0 = (2.81 \pm 0.23) \text{ mg L}^{-1}$ ;  $[\text{DFZ}]_0 = (1.86 \pm 0.16) \text{ mg L}^{-1}$ ;  $[\text{IMD}]_0 = (2.71 \pm 0.19) \text{ mg L}^{-1}$

$$k_{\text{DFZ}} = -0.12759 + 0.00733x_1 + 0.01435x_2 - 0.00003x_1^2 \quad (10)$$

$$k_{\text{IMD}} = -0.62688 + 0.00133x_1 + 0.071654x_2 - 0.00129x_2^2 \quad (11)$$

### Application of the UVC/ $\text{H}_2\text{O}_2$ process to the treatment of real rinse water

Figure 7 presents the results of the experiments carried out with real tomato rinse water sampled in the industry (pre-washing and washing belts), spiked with the commercial products Amistar Top® and Provado 200 SC®, submitted to the UVC/ $\text{H}_2\text{O}_2$  treatment with  $[\text{H}_2\text{O}_2]_0 = 130 \text{ mg L}^{-1}$  and  $E_{\text{UVC}} = 28.6 \text{ W m}^{-2}$ , i.e., the optimum conditions determined from the Doehlert design. Both aqueous matrices absorb UVC radiation at 254 nm, while the water generated in the pre-washing operation has a high content of TOC and solids (Table S1).

Despite these characteristics, complete removal of AZO was achieved for both matrices after 15 min, while the total degradation of DFZ and IMD was obtained only for the water collected in the washing belts; in contrast, removals of about 70% and 79% were achieved for DFZ and IMD, respectively, for the water generated in the pre-washing operation.

The corresponding pseudo-first-order specific degradation rates were  $k_{\text{AZO}} = 0.128 \pm 0.002 \text{ s}^{-1}$  ( $R^2 = 0.902$ ),  $k_{\text{DFZ}} = 0.025 \pm 0.005 \text{ s}^{-1}$  ( $R^2 = 0.985$ ), and  $k_{\text{IMD}} = 0.129 \pm 0.004 \text{ s}^{-1}$  ( $R^2 = 0.995$ ) (pre-washing water) and  $k_{\text{AZO}} = 0.249 \pm 0.004 \text{ s}^{-1}$  ( $R^2 = 0.928$ ),  $k_{\text{DFZ}} = 0.055 \pm 0.001 \text{ s}^{-1}$  ( $R^2 = 0.997$ ), and  $k_{\text{IMD}} = 0.266 \pm 0.022 \text{ s}^{-1}$  ( $R^2 = 0.994$ ) (washing belts water). Compared with the  $k$ -values obtained for the synthetic rinse water (Figure S15), these values confirm that the water matrix does not influence AZO removal, unlike DFZ and IMD. Therefore, aiming at the complete removal of the active ingredients after 15 min, the UVC/ $\text{H}_2\text{O}_2$  process can be considered a viable alternative for the treatment of the rinse water generated in the washing belts.

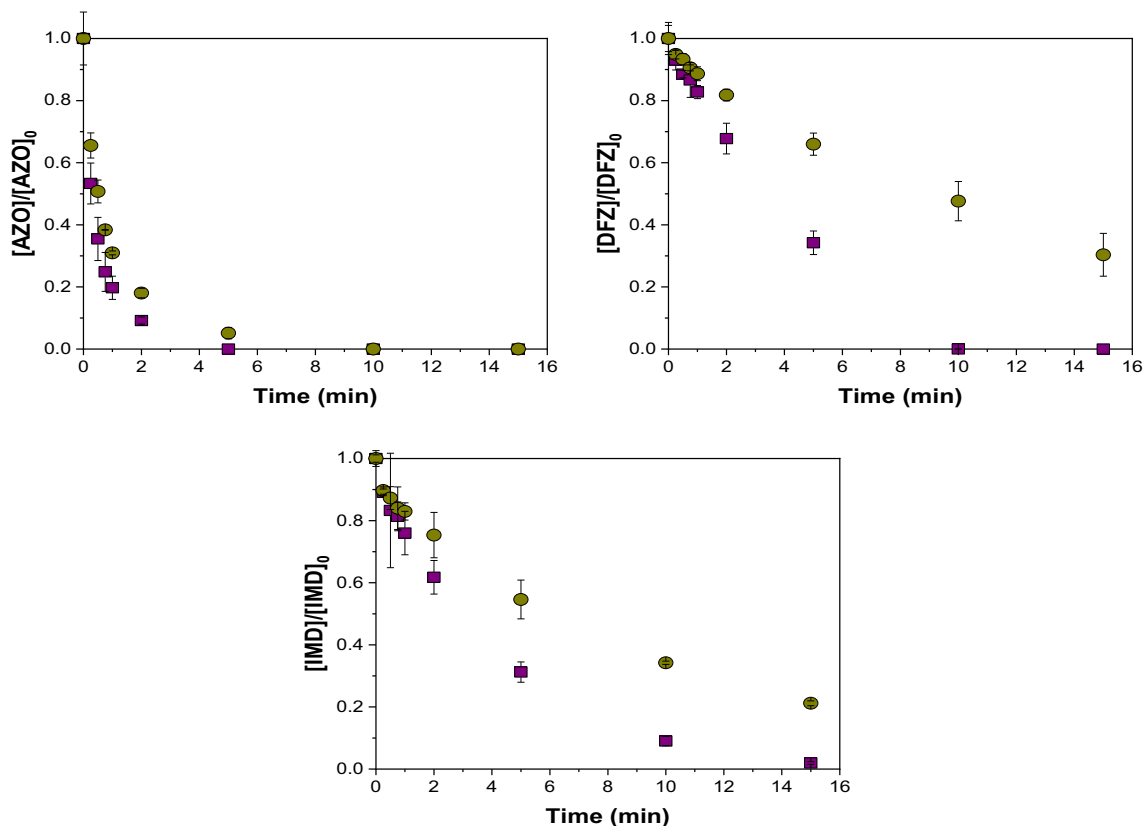


**Fig. 7** AZO, DFZ, and IMD decay over time for the experiments carried out with rinse water sampled in the industry, spiked with the commercial products Amistar Top® and Provado 200 SC® and submitted to the UVC/H<sub>2</sub>O<sub>2</sub> treatment with [H<sub>2</sub>O<sub>2</sub>]<sub>0</sub> = 130 mg L<sup>-1</sup> and E<sub>UVC</sub> = 28.6 W

m<sup>-2</sup>. Washing belts water (violet square); pre-washing water (brown circle). [AZO]<sub>0</sub> = 2.22 ± 0.05 mg L<sup>-1</sup>; [DFZ]<sub>0</sub> = 1.48 ± 0.04 mg L<sup>-1</sup>; [IMD]<sub>0</sub> = 2.94 ± 0.14 mg L<sup>-1</sup> mg L<sup>-1</sup>. The average errors are 5.5% (AZO), 13.9% (DFZ), and 2.8% (IMD)

### Cytotoxicity and genotoxicity of untreated and treated real rinse water

The cytotoxicity and genotoxicity tests were performed using the test organism *A. cepa*, which has been found to be suitable for environmental monitoring and is recognized as a toxicity bioindicator by the International Programme on Chemical Safety of the United Nations (WHO 1985) and the United States Environmental Protection Agency (USEPA 1996), due to its high sensitivity to chemical compounds and the presence of a small number of large chromosomes (2n = 16), which allows to check the damage to cell DNA, such as chromosome anomalies. In addition, it is a test of easy applicability and low cost and has shown reliable results in the analysis of several compounds, among which several pesticides (Leme and Marin-Morales 2009).

The results of the tests performed with real tomato rinse water sampled in the industry (pre-washing and washing belts) are presented in Table 2 and Fig. 8. These matrices were previously fortified with Amistar Top® and Provado 200 SC® and then treated by the UVC/H<sub>2</sub>O<sub>2</sub> process in the optimum conditions mapped by the Doehlert design ([H<sub>2</sub>O<sub>2</sub>]<sub>0</sub> = 130 mg L<sup>-1</sup>; E<sub>UVC</sub> = 28.6 W m<sup>-2</sup>). For both untreated water

samples (Fig. 8b and c), a decrease in the rate of cell division was observed, resulting in a lower mitotic index compared to that of the control (Fig. 8a). According to Leme and Marin-Morales (2009), MI values lower than those of the control may indicate changes in the growth and development of the cells, due to the exposure to pesticides. The UVC/H<sub>2</sub>O<sub>2</sub> treatment, although not able to completely remove all the pesticides from pre-washing rinse water, proved to be efficient to

**Table 2** Mitotic index (MI) of the root meristem cells of *Allium cepa* (× 40 magnification), performed with real tomato rinse water sampled in the industry, spiked with the commercial products Amistar Top® and Provado 200 SC®, and submitted to the UVC/H<sub>2</sub>O<sub>2</sub> treatment at the optimum conditions of [H<sub>2</sub>O<sub>2</sub>]<sub>0</sub> = 130 mg L<sup>-1</sup> and E<sub>UVC</sub> = 28.6 W m<sup>-2</sup> indicated by the Doehlert design

| Assay  | MI (%)     |
|--|------------|
| Negative control (tap water)   | 74.7 ± 6.2 |
| Pre-washing water, untreated   | 66.3 ± 5.2 |
| Washing belts water, untreated   | 52.9 ± 4.2 |
| Pre-washing water, after the UVC/H <sub>2</sub> O <sub>2</sub> treatment   | 74.8 ± 6.3 |
| Washing belts water, after the UVC/H <sub>2</sub> O <sub>2</sub> treatment | 77.6 ± 4.0 |

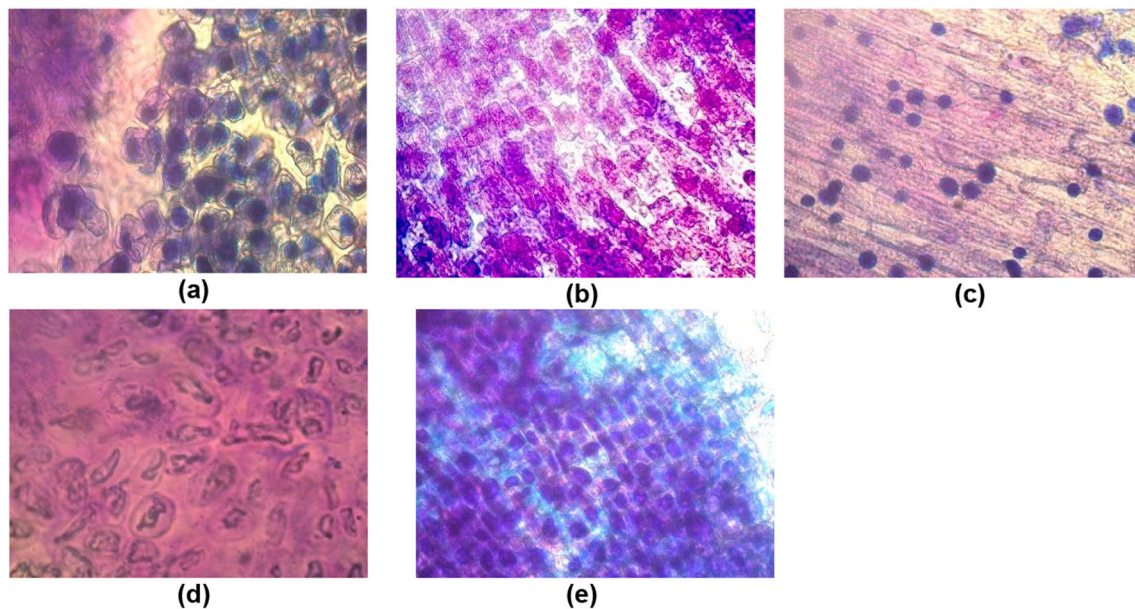


**Fig. 8** Results of the genotoxic assays with *Allium cepa* ( $\times 40$  magnification), performed with real tomato rinse water sampled in the industry. **a** Negative control (tap water); **b** pre-washing water, untreated; **c**

washing belts water, untreated; **d** pre-washing water, after the UVC/H<sub>2</sub>O<sub>2</sub> treatment; **e** washing belts water, after the UVC/H<sub>2</sub>O<sub>2</sub> treatment

improve the MI values. Regarding the genotoxic effects, abnormal cells were observed, with micronuclei found for the pre-washing water before treatment (Fig. 8b), which is associated with a decrease in cell division, confirmed by the lower MI value. According to Fernandes et al. (2007), the occurrence of micronuclei is generally understood as an indication of damage to the genetic material when exposed to mutagenic agents, although they can occur spontaneously. In addition, telophasic bridges were present in the cells after the application of the UVC/H<sub>2</sub>O<sub>2</sub> treatment (Fig. 8d).

These results emphasize the importance of analyzing both effects in toxicological tests, because, although the cells exposed to treated pre-washing rinse water had MI values close to that of the negative control, the rate of cell division being similar to the control does not guarantee that chromosome anomalies are absent; this effect is probably due to the presence of remaining parent compound molecules and/or their transformation intermediates. In contrast, for the water collected in the washing belts, the three active ingredients were completely removed after 15 min by the UVC/H<sub>2</sub>O<sub>2</sub> treatment, and the test showed that no abnormalities occurred during cell division (Fig. 8e). Thus, although the MI was slightly higher than that observed for the negative control, the cells were healthy, confirming the efficiency of the treatment process from a toxicological point of view. In any case, in order to better understand how the target pesticides and their degradation intermediates contribute to the observed effects, further investigations on their transformation route in aqueous media are needed.

Few studies are found in the literature in which the cytotoxic and genotoxic effects of DFZ and IMD were investigated, alone or in the mixture, using *A. cepa*. Bernardes et al. (2015) observed

phytotoxic, cytotoxic, and genotoxic effects of DFZ after 96 h of exposure to concentrations ranging from 7.81 to 125.0  $\mu\text{g L}^{-1}$  and found a decrease in MI and an increase in the incidence of chromosome anomalies in cells with increasing DFZ concentration. In addition, it has been observed that despite the greatest phytotoxic damage occurring at higher concentrations, DFZ causes mutations in DNA more frequently at residual concentrations. Bianchi et al. (2016) investigated the individual effects of IMD and in mixture with the herbicide sulfentrazone and after 24 h of exposure, observing indirect genotoxic effects of IMD, with the presence of chromosome anomalies, in most cases consisting in bridges and adhesions. In the mixture, the two compounds showed genotoxic and cytotoxic effects, reducing the MI value. The same genotoxic behavior of IMD was observed by Fioresi et al. (2020), with more concentrated solutions causing a reduction in the mitotic index. In contrast, no studies have been reported for AZO using the test organism *A. cepa*, which highlights the contribution of the present study not only with regard to the applicability of the UVC/H<sub>2</sub>O<sub>2</sub> process in the treatment of real rinse water but also to the toxicological reduction potential of this technology.

## Conclusions

The results of the present study demonstrate that the UVC direct photolysis of azoxystrobin (AZO), difenoconazole (DFZ), and imidacloprid (IMD), pesticides commonly found in the tomato rinse water generated through washing operations in the industry, follows pseudo-first-order kinetics, with AZO and IMD reaching concentrations below the respective

detection limits after 15-min irradiation at 21.8 and 28.6 W m<sup>-2</sup>. In contrast, only 51.7% removal was obtained for DFZ, using 28.6 W m<sup>-2</sup>. The highest photolysis quantum yield in the wavelength range 251–257 nm was obtained for AZO ( $\Phi_{\text{AZO}} = 0.572 \text{ mol Einstein}^{-1}$ ), which is one order of magnitude higher than those found for DFZ (0.028 mol Einstein<sup>-1</sup>) and IMD ( $\Phi_{\text{IMD}} = 0.061 \text{ mol Einstein}^{-1}$ ).

With regard to UVC/H<sub>2</sub>O<sub>2</sub>, total pesticide removal was achieved in the first 10 min for most conditions of [H<sub>2</sub>O<sub>2</sub>]<sub>0</sub> and irradiance ( $E_{\text{UVC}}$ ). The results also suggest that the contribution of direct photolysis to the initial rate of pesticide degradation during the UVC/H<sub>2</sub>O<sub>2</sub> process followed the order IMD > AZO > DFZ, which is expected, given the competition between H<sub>2</sub>O<sub>2</sub> and pesticides molecules for incident photons. In this case, the statistical analysis using the sequential Doehlert design enabled a better understanding of the influence of the process variables. In fact, [H<sub>2</sub>O<sub>2</sub>]<sub>0</sub> was shown to be more influential on AZO and DFZ removal rates, while IMD degradation seemed to be more impacted by irradiance. Moreover, the negative quadratic effect of  $E_{\text{UVC}}$  was statistically significant for AZO and IMD, whilst [H<sub>2</sub>O<sub>2</sub>]<sub>0</sub> was significant for DFZ, at the 95% confidence level. The quadratic response surface models confirmed that the optimum conditions, regarding pesticide removal rates, were about [H<sub>2</sub>O<sub>2</sub>]<sub>0</sub> = 130 mg L<sup>-1</sup> and  $E_{\text{UVC}}$  = 26 W m<sup>-2</sup>.

Under these conditions, complete removal of AZO was achieved for real tomato rinse water sampled in the industry (pre-washing and washing belts), spiked with the commercial pesticides, while the total degradation of DFZ and IMD was obtained only for the water collected in the washing belts; in contrast, removals of about 70% and 79% were achieved for DFZ and IMD, respectively, for the water generated in the pre-washing operation. Although the cells of *A. cepa* exposed to treated pre-washing rinse water had mitotic index values close to that of the negative control (tap water), chromosome anomalies were identified, which is probably due to the presence of remaining parent compound molecules and/or their transformation intermediates. In contrast, for the water collected in the washing belts, the three active ingredients were completely removed after 15 min by the UVC/H<sub>2</sub>O<sub>2</sub> treatment, with no abnormalities observed during cell division. Therefore, the UVC/H<sub>2</sub>O<sub>2</sub> process can be considered a viable alternative for the localized treatment of rinse water generated in the washing belts during tomato processing in the industry, with a focus on the possible reuse of treated water.

**Supplementary Information** The online version contains supplementary material available at <https://doi.org/10.1007/s11356-021-13387-7>.

**Acknowledgments** The authors are also grateful to the National Council for Scientific and Technological Development (CNPq), to the agrochemical engineers from Emater-MG for providing essential information about the pesticides used in tomato cultivation, to P. Metolina for the support with the calculation of photolysis quantum yields, and to N. Klanovicz for the support with cytotoxicity and genotoxicity assays with *Allium cepa*.

**Author contributions** I.L.C.C.: conceptualization, methodology, validation, formal analysis, investigation, writing—original draft, visualization.

A.C.S.C.T.: conceptualization, validation, resources, writing—original draft, writing—review & editing, supervision, funding acquisition.

All authors read and approved the final manuscript.

**Funding** This study was financed in part by the Coordenação de Aperfeiçoamento de Pessoal de Nível Superior - Brasil (CAPES - Coordination for the Improvement of Higher Education Personnel) – Finance Code 001, National Council for Scientific and Technological Development (CNPq, grant #307481/2017-4) and São Paulo Research Foundation (FAPESP, grant #2018/21271-6).

**Data Availability** All data generated or analyzed during this study are included in this published article and its supplementary information file.

## Declarations

**Ethics approval and consent to participate** Not applicable.

**Consent for publication** Not applicable.

**Competing interests** The authors declare that they have no competing interests.

## References

- Aliste M, Pérez-Lucas G, Vela N, Garrido I, Fenoll J, Navarro S (2020) Solar-driven photocatalytic treatment as sustainable strategy to remove pesticide residues from leaching water. *Environ Sci Pollut Res* 27:7222–7233. <https://doi.org/10.1007/s11356-019-07061-2>
- Al-Rimawi F (2016) A HPLC-UV method for determination of three pesticides in water. *Int J Adv Chem* 2:1–8. <https://doi.org/10.5121/ijac.2016.2102>
- Ameta SC (2018) Introduction. In: Ameta SC, Ameta R (eds) *Advanced oxidation processes for wastewater treatment: emerging green chemical technology*. Elsevier, London, pp 1–8
- Andrade GCRM, Monteiro SH, Francisco JG et al (2015) Effects of types of washing and peeling in relation to pesticide residues in tomatoes. *J Braz Chem Soc* 26:1994–2002. <https://doi.org/10.5935/0103-5053.20150179>
- Baghirzade BS, Yetis U, Dilek FB (2020) Imidacloprid elimination by O<sub>3</sub> and O<sub>3</sub>/UV: kinetics study, matrix effect, and mechanism insight. *Environ Sci Pollut Res*. <https://doi.org/10.1007/s11356-020-09355-2>
- Barbosa MO, Moreira NFF, Ribeiro AR, Pereira MFR, Silva AMT (2016) Occurrence and removal of organic micropollutants: an overview of the watch list of EU Decision 2015/495. *Water Res* 94:257–279. <https://doi.org/10.1016/j.watres.2016.02.047>
- Bernardes PM, Andrade-Vieira LF, Aragão FB, Ferreira A, da Silva Ferreira MF (2015) Toxicity of difenoconazole and tebuconazole in *Allium cepa*. *Water Air Soil Pollut* 226:207. <https://doi.org/10.1007/s11270-015-2462-y>
- Bessergenev VG, Mateus MC, Morgado IM, Hantusch M, Burkel E (2017) Photocatalytic reactor, CVD technology of its preparation and water purification from pharmaceutical drugs and agricultural pesticides. *Chem Eng J* 312:306–316. <https://doi.org/10.1016/j.cej.2016.11.148>
- Bethi B, Sonawane SH, Bhavas BA, Gumbert SP (2016) Nanomaterials-based advanced oxidation processes for wastewater treatment: a

- review. *Chem Eng Process* 109:178–189. <https://doi.org/10.1016/j.cep.2016.08.016>
- Bianchi J, Fernandes TCC, Marin Morales MA (2016) Induction of mitotic and chromosomal abnormalities on *Allium cepa* cells by pesticides imidacloprid and sulfentrazone and the mixture of them. *Chemosphere*. 144:475–483. <https://doi.org/10.1016/j.chemosphere.2015.09.021>
- Bolton JR, Bircher KG, Tumas W, Tolman CA (2001) Figures-of-merit for the technical development and application of advanced oxidation technologies for both electric- and solar-driven systems (IUPAC Technical Report). *Pure Appl Chem* 73:627–637. <https://doi.org/10.1351/pac200173040627>
- Bombardi LM (2017) Geografia do uso de agrotóxicos no Brasil e conexões com a União Europeia. FFLCH-USP, São Paulo
- Boudina A, Emmelin C, Baaliouamer A, Païssé O, Chovelon JM (2007) Photochemical transformation of azoxystrobin in aqueous solutions. *Chemosphere* 68:1280–1288. <https://doi.org/10.1016/j.chemosphere.2007.01.051>
- Braun AM, Maurette MT, Oliveros E (1991) Photochemical technology. Wiley, Chichester
- Caldas LFS, Paula CER, Brum DM, Cassella RJ (2012) Application of a four-variables Doehlert design for the multivariate optimization of copper determination in petroleum-derived insulating oils by GFAAS employing the dilute-and-shot approach. *Fuel* 105:503–511. <https://doi.org/10.1016/j.fuel.2012.10.026>
- Caldas SS, Bolzan CM, Guilherme JR, Silveira MAK, Escarrone ALV, Primel EG (2013) Determination of pharmaceuticals, personal care products, and pesticides in surface and treated waters: method development and survey. *Environ Sci Pollut Res* 20:5855–5863. <https://doi.org/10.1007/s11356-013-1650-9>
- Calza P, Medana C, Baiocchi C, Pelizzetti E (2006) Light-induced transformations of fungicides on titanium dioxide: pathways and by-products evaluation using the LC-MS technique. *Int J Environ Anal Chem* 86:267–275. <https://doi.org/10.1080/03067310500247959>
- Fast SA, Gude VG, Truax DD, Martin J, Magbanua BS (2017) A critical evaluation of advanced oxidation processes for emerging contaminants removal. *Environ Process* 4:283–302. <https://doi.org/10.1007/s40710-017-0207-1>
- Fenoll J, Garrido I, Hellín P, Flores P, Navarro S (2015) Photodegradation of neonicotinoid insecticides in water by semiconductor oxides. *Environ Sci Pollut Res* 22:15055–15066. <https://doi.org/10.1007/s11356-015-4721-2>
- Fernandes TCC, Mazzeo DEC, Marin-Morales MA (2007) Mechanism of micronuclei formation in polyploidized cells of *Allium cepa* exposed to trifluralin herbicide. *Pestic Biochem Physiol* 88:252–259. <https://doi.org/10.1016/j.pestbp.2006.12.003>
- Ferreira SLC, Santos WNL, Quintella CM et al (2004) Doehlert matrix: a chemometric tool for analytical chemistry: review. *Talanta* 63:1061–1067. <https://doi.org/10.1016/j.talanta.2004.01.015>
- Fiorenza R, Balsamo SA, D’Urso L, Sciré S, Brundo MV, Pecoraro R, Scalisi EM, Privitera V, Impellizzeri G (2020) CeO<sub>2</sub> for water remediation: comparison of various advanced oxidation processes. *Catalysts* 10:446. <https://doi.org/10.3390/catal10040446>
- Fioresi VS, Vieira BCR, Campos JMS et al (2020) Cytogenotoxic activity of the pesticides imidacloprid and iprodione on *Allium cepa* root meristem. *Environ Sci Pollut Res* 27:28066–28076. <https://doi.org/10.1007/s11356-020-09201-5>
- Fiskesjö G (1985) The *Allium* test as a standard in environmental monitoring. *Hereditas* 102:99–112. <https://doi.org/10.1111/j.1601-5223.1985.tb00471.x>
- Garrido et al (2020) Solar reclamation of agro-wastewater polluted with eight pesticides by heterogeneous photocatalysis using a modular facility. A case study. *Chemosphere* 249:126–156. <https://doi.org/10.1016/j.chemosphere.2020.126156>
- Han Y, Liu T, Wang J, Wang J, Zhang C, Zhu L (2016) Genotoxicity and oxidative stress induced by the fungicide azoxystrobin in zebrafish (*Danio rerio*) livers. *Pestic Biochem Physiol* 133:13–19. <https://doi.org/10.1016/j.pestbp.2016.03.011>
- Kanwal M, Tariq SR, Chotana GA (2018) Photocatalytic degradation of imidacloprid by Ag-ZnO composite. *Environ Sci Pollut Res* 25:27307–27320. <https://doi.org/10.1007/s11356-018-2693-8>
- Katsoyiannis IA, Canonica S, Von Gunten U (2011) Efficiency and energy requirements for the transformation of organic micropollutants by ozone, O<sub>3</sub>/H<sub>2</sub>O<sub>2</sub> and UV/H<sub>2</sub>O<sub>2</sub>. *Water Res* 45:3811–3822. <https://doi.org/10.1016/j.watres.2011.04.038>
- Lastre-Acosta AM, Vicente R, Mora M, Jáuregui-Haza UJ, Arques A, Teixeira ACSC (2019) Photo-Fenton reaction at mildly acidic conditions: assessing the effect of bio-organic substances of different origin and characteristics through experimental design. *J Environ Sci Health A Tox Hazard Subst Environ Eng* 54:711–720. <https://doi.org/10.1080/10934529.2019.1585721>
- Leme DM, Marin-Morales MA (2009) *Allium cepa* test in environmental monitoring: a review on its application. *Mutat Res* 682:71–81. <https://doi.org/10.1016/j.mrrev.2009.06.002>
- Li Y, Ma X, Lu G (2013) Systematic investigation of the toxic mechanism of difenoconazole on protein by spectroscopic and molecular modeling. *Pestic Biochem Physiol* 105:155–160. <https://doi.org/10.1016/j.pestbp.2012.12.010>
- MAPA (2020) Informações técnicas. <http://www.agricultura.gov.br/assuntos/insumos-agropecuarios/insumos-agricolas/agrotoxicos/informacoes-tecnicas>. Accessed 29 June 2020
- Maurya R, Dubey K, Singh D, Jain AK, Pandey AK (2019) Effect of difenoconazole fungicide on physiological responses and ultrastructural modifications in model organism *Tetrahymena pyriformis*. *Ecotoxicol Environ Saf* 182:109–375. <https://doi.org/10.1016/j.ecoenv.2019.109375>
- Mierzwa JC, Rodrigues R, Teixeira ACSC (2018) UV-hydrogen peroxide processes. In: Ameta SC, Ameta R (eds) *Advanced oxidation processes for wastewater treatment: emerging green chemical technology*. Elsevier, London, pp 13–48
- Miklos DB, Remy C, Jekel M, Linden KG, Drewes JE, Hübner U (2018) Evaluation of advanced oxidation processes for water and wastewater treatment: a critical review. *Water Res* 139:118–131. <https://doi.org/10.1016/j.watres.2018.03.042>
- Monsalvo VM, Garcia-Mancha N, Puyol D, Mohedano AF, Rodriguez JJ (2014) Anaerobic biodegradability of mixtures of pesticides in an expanded granular sludge bed reactor. *Water Sci Technol* 69:532–538. <https://doi.org/10.2166/wst.2013.739>
- Navarro S, Fenoll J, Vela N, Ruiz E, Navarro G (2011) Removal of tem pesticides from leaching water at pilot plant scale by photo-Fenton treatment. *Chem Eng J* 167:42–49. <https://doi.org/10.1016/j.cej.2010.11.105>
- Novaes CG, Yamaki RT, De Paula VF, Do Nascimento Júnior BB, Barreto JA, Velasques GS, Bezerra MA (2017) Otimização de métodos analíticos usando metodologia de superfícies de resposta - Parte I: variáveis de processo. *Rev Virtual Quim* 9:1184–1215
- Oppenländer T (2003) Photochemical purification of water and air. Wiley-VCH, Weinheim
- Pan L, Lu L, Wang J, Zheng C, Fu Y, Xiao S, Jin Y, Zhuang S (2017) The fungicide difenoconazole alters mRNA expression levels of human CYP3A4 in HepG2 cells. *Environ Chem Lett* 15:673–678. <https://doi.org/10.1007/s10311-017-0636-0>
- Parsons S (2005) *Advanced oxidation processes for water and wastewater treatment*. IWA Publishing, London
- Pushkareva TI, Zenkevich IG (2018) Electrochemical oxidation of difenoconazole in solutions: LC/MS identification of reaction products. *Mosc Univ Chem Bull* 74:127–133. <https://doi.org/10.3103/S0027131419030106>

- Ribani M, Bottoli CBG, Collins CH, Jardim ICSF, Melo LFC (2004) Validação em métodos cromatográficos e eletroforéticos. *Quim Nova* 27:771–780
- Rodrigues AAZ, De Queiroz MELR, De Oliveira AF et al (2017) Pesticide residue removal in classic domestic processing of tomato and its effects on product quality. *J Environ Sci Health B* 52:1–8. <https://doi.org/10.1080/03601234.2017.1359049>
- Rózsa G, Náfrádi M, Alapi T, Schrantz K, Szabó L, Wojnárovits L, Takács E, Tungler A (2019) Photocatalytic, photolytic and radiolytic elimination of imidacloprid from aqueous solution: reaction mechanism, efficiency and economic considerations. *Appl Catal B Environ* 250:429–439. <https://doi.org/10.1016/j.apcatb.2019.01.065>
- Segura C, Zaror C, Mansilla H, Mondaca M (2008) Imidacloprid oxidation by photo-Fenton reaction. *J Hazard Mater* 150:679–686
- Sena AR, Valasques Júnior GL, Barretto IKSP, Assis SA (2012) Application of doehlert experimental design in the optimization of experimental variables for the *pseudozyma* sp. (CCMB 306) and *pseudozyma* sp. (CCMB 300) cell lysis. *Cienc Tecnol Aliment* 32:761–767. <https://doi.org/10.1590/S0101-20612012005000118>
- Silva MB, Nocelli RCF, Soares HM, Malaspina O (2016) Efeitos do imidacloprido sobre o comportamento das abelhas *Scaptotrigona postica* Latreille, 1807 (Hymenoptera, Apidae). *Rev Ciên Tec Amb* 3:21–28
- Skoog DA, Holler FJ, Crouch SR (2017) Principles of instrumental analysis. Cengage Learning, Boston
- Tang WZ (2004) Physicochemical treatment of hazardous wastes. CRC Press LLC, Florida
- Tišler T, Jemec A, Mozetič B, Trebše P (2009) Hazard identification of imidacloprid to aquatic environment. *Chemosphere* 76:907–914. <https://doi.org/10.1016/j.chemosphere.2009.05.002>
- Todey SA, Fallon AM, Arnold WA (2018) Neonicotinoid insecticide hydrolysis and photolysis: rates and residual toxicity. *Environ Toxicol Chem* 37:2797–2809. <https://doi.org/10.1002/etc.4256>
- Tsochatzis ED, Tzimou-Tsitouridou R, Menkissoglu-Spiroudi U, Karpouzias DG, Papageorgiou M (2011) Development and validation of an HPLC-DAD method for the simultaneous determination of most common rice pesticides in paddy water systems. *Int J Environ Anal Chem* 92:548–560. <https://doi.org/10.1080/03067310903229943>
- US Environmental Protection Agency (USEPA) (1996) Seed germination/root elongation toxicity test, OPPTS 50.4200, EPA 712/C-96/154. Ecological effects test guidelines. Washington, DC
- World Health Organization (1985) Guide to short-term tests for detecting mutagenic and carcinogenic chemicals. *Environ Health Criteria* 51, Geneva, pp. 208
- Yaqub G, Iqbal K, Sadiq Z, Hamid A (2017) Rapid determination of residual pesticides and polyaromatic hydrocarbons in different environmental samples by HPLC. *Pak J Agric Sci* 54:355–361. <https://doi.org/10.21162/PAKJAS/17.5057>
- Zapata A, Oller I, Sirtori C, Rodríguez A, Sánchez-Pérez JA, López A, Mezcua M, Malato S (2010) Decontamination of industrial wastewater containing pesticides by combining large-scale homogeneous solar photocatalysis and biological treatment. *Chem Eng J* 160:447–456. <https://doi.org/10.1016/j.cej.2010.03.042>
- Zheng W, Liu W, Wen Y, Sang-Jin L (2004) Photochemistry of insecticide imidacloprid: direct and sensitized photolysis in aqueous medium. *J Environ Sci* 16:539–542

**Publisher's note** Springer Nature remains neutral with regard to jurisdictional claims in published maps and institutional affiliations.